

# A self-adaptative oscillator

A. Boudaoud<sup>a</sup>, Y. Couder, and M. Ben Amar

Laboratoire de Physique Statistique, École Normale Supérieure, 24 rue Lhomond, 75231 Paris Cedex 05, France

Received 15 October 1998

**Abstract.** The dynamics of a system where a mass is free to slide on a vibrating string is investigated as the excitation frequency is varied. One degree of freedom is thus added to the system studied by Helmholtz in which a mass was fixed on a vibrating string. This new system exhibits a specific dynamics characterized by the existence of a self-adaptative behaviour. When the driving frequency falls into wide and well defined frequency bands, a long transient is observed by which the mass adjusts its position so that the whole system becomes resonant. In the gaps between these bands, bifurcations give other equilibrium positions. A theoretical model is proposed. It accounts for all the experimental results. In the case where two masses are present on the string, two degrees of freedom are added and the set of equilibrium positions would be expected to be infinite. However, in the experiment, the two masses are observed to go to positions where they are symmetrical with respect to the middle of the string. A selection mechanism due to the string stretching is pointed out.

**PACS.** 47.20.Ky Nonlinearity (including bifurcation theory) – 68.45.Kg Dynamics; vibrations

## 1 Introduction

Vibrating strings have been widely investigated during the nineteenth century. Several problems in this domain were more difficult than it might seem now that it has become a topic for textbooks. For instance, there was a strong debate between Euler, d'Alembert and Lagrange [1] on the possibility of a slope discontinuity for a plucked string. Lagrange [1] also examined the non-harmonic vibrations of a string with a variable density. Helmholtz [2] wanted to determine the lower frequencies that a human being can hear. For this purpose, he studied the basic frequencies of a string loaded with one fixed point-like mass. Helmholtz calculations give the eigenfrequencies of the system as a function of the mass position along the string. It was pointed out recently by Brazovskaia and Pieranski [3] that this problem is equivalent to a quantum billiard with a pointlike scatterer. However, these studies were only concerned with the eigenmodes of the perturbed system. The present letter is devoted to the study of a string loaded with point-like masses which are free to slide. We will show that this system, when forced by an external frequency belonging to large frequency bands, self-adapts to remain resonant.

The self adaptation of a vibrating system to a forcing frequency was previously found in two systems. In an unpublished work [4], Airiau, Couder and Rabaud observed that when a thick soap film is forced into vibration by a loudspeaker, the film retains a large amplitude of oscillation in very wide ranges of frequency. A characteris-

tic of soap films is that their thickness can vary spatially and that the film is liquid. When forced into vibration, the fluid flows in such a way that in the steady regime the mass is very unevenly distributed. With an elongated rectangular frame, at a frequency corresponding to the  $n$ th eigenmode, most of the film mass is concentrated in the  $n$  antinodes. When the frequency is increased the mass distribution changes continuously so that the vibration amplitude remains large. Eventually, the mass in each antinode splits and the film is reorganized so as to have mass concentrated in the  $n + 1$  antinodes of the next mode. Independently, Brazovskaia *et al.* [5] performed experiments with square smectic films of uneven thickness. They found that the film thickens at the vibration antinode. A peninsula consisting of many layers of smectic appears at the antinode and its shape adapts to the forcing. However, smectic films of constant thickness are also easily obtained; in this latter case, they are perfect membranes with eigenfrequencies following the Rayleigh law [6]. Brazovskaia and Pieranski [3] also observed a self-tuning property: when a smectic film is loaded with a small bead, it adjusts its position with the forcing frequency. The aim of the present work is to find this type of nonlinear behaviour in a model system, such that both the experiment and the theory can be extensively tractable.

## 2 The experimental setup

The experimental apparatus is very simple: we thread one or two beads on a string and force the oscillation of the system magnetically. The qualities of music instruments led us to use a piano string made of 0.5 mm diameter

---

<sup>a</sup> e-mail: boudaoud@lps.ens.fr

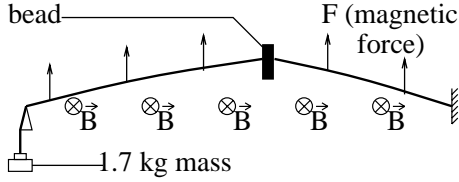


**Fig. 1.** Scheme of the experimental apparatus. A piano string fixed at one end is tightened horizontally with a mass at the other end. The magnetic field is generated by two U-shaped magnets and two iron plates. An alternating current passes through the string.

steel with a mass per unit length  $\lambda = 1.53$  g/m. The useful string length was chosen to be  $L = 30$  cm. With a smaller length, the bead position is not measured precisely enough, while with a larger length, it is difficult to obtain a homogeneous magnetic field for the forcing. The total string mass is  $\lambda L = 0.46$  g. The string is held horizontally and tightened with a mass giving a tension  $T = 17$  N (Fig. 1).

The beads are small disks of masses  $m = 0.21$  g,  $0.73$  g and  $1.82$  g. They are pierced by holes of  $0.55$  mm diameter, slightly larger than the string diameter. Once threaded on the string, the bead can thus have a small amplitude bouncing motion. This suppresses the possibility of a solid friction which could block the motion. Provided the amplitude of the bouncing remains very small compared with that of the oscillation, it does not introduce any artefact into the experiment. The results are identical to those obtained when the bead slides on the string with a pure viscous friction [7]. When the hole was drilled through the center of the disk, the bead spun and there was a coupling between vibration and rotation. To prevent the spinning, the hole was drilled off-centered so that the disk forms a little pendulum. The hole position and the disk size were chosen so that the bead oscillation frequencies would be very large compared to the imposed frequencies. We thus avoid any coupling between the disk's oscillations and the string's vibration.

In order to have a spatially homogeneous system, we chose a magnetic forcing where the force exerted on the wire is the same everywhere. An alternating current (1 to 10 A) of tunable frequency passes through the string. This string is located between the poles of two identical U-shaped permanent magnets generating a horizontal magnetic field. Since we wish this magnetic field to be spatially constant, two long and thick iron plates are interposed, parallel to each other and located between the poles and the wire. Since iron channels the magnetic flux, the field which is directed from one plate to the other (Fig. 1) is thus spread out and approximately constant along all the length of the wire ( $B \sim 0.1$  T). The magnetic force is vertical and can go up to 1 N/m. The excitation was not perfect, the magnetic field still had slight variations along the string. For reasons discussed below, we also used a configuration where the magnetic field has its sign reversed at the middle of the string. The driving amplitude or

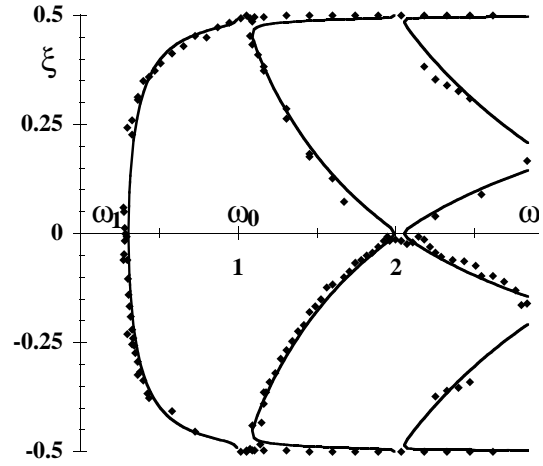


**Fig. 2.** The nondimensional steady positions of the bead as a function of the forcing frequency (the unit of frequencies being the fundamental frequency  $\omega_0$  of the unloaded string). The diamonds result from an experiment done with a bead of mass  $m = 1.82$  g. The different steady positions at a given frequency were measured in independent realizations. The curves are the predicted positions of equilibrium (solutions of Eq. (12)) for the corresponding mass ratio  $\mu = 4$ .

frequency are easily adjusted with a function generator and measured with a frequency counter and an oscilloscope.

### 3 Experimental results

We first investigated the resonances of the string alone. Its fundamental frequency is  $\omega_0 = 126$  Hz. We measured the amplitude of vibration as a function of the frequency. A ruler gives a precision of  $0.5$  mm on the amplitude. The resonance width is of the order of  $\gamma \approx 5$  Hz, so damping is small. There is hysteresis in the response curve, as for a 1D nonlinear oscillator. Thus, the amplitude of vibration is imposed by the nonlinearities and the damping may be neglected.

#### 3.1 With a single bead

A single bead is now placed on the string. We first describe the results obtained with a bead of mass  $m = 1.82$  g, heavier than the string ( $\mu = m/\lambda L = 4.0$ ). The bead is first placed arbitrarily on the string and the system is forced at a frequency  $\omega$ . For most frequencies, when the forcing is switched on, a slow evolution is observed where the mass slides along the wire and the oscillations change. Ultimately a steady regime is reached. We then measure the bead position  $\xi$ . It is obtained with a precision of  $1$  mm, *i.e.*  $1/300$  of the string length, while the precision on frequency is  $0.1$  Hz, *i.e.* less than  $1/1000$  of the basic frequency. We then repeat the same operation varying the forcing frequency step by step so as to obtain the evolution of  $\xi$  as a function of  $\omega$ . The experimental results are shown in Figure 2 on which, for the sake of comparison with

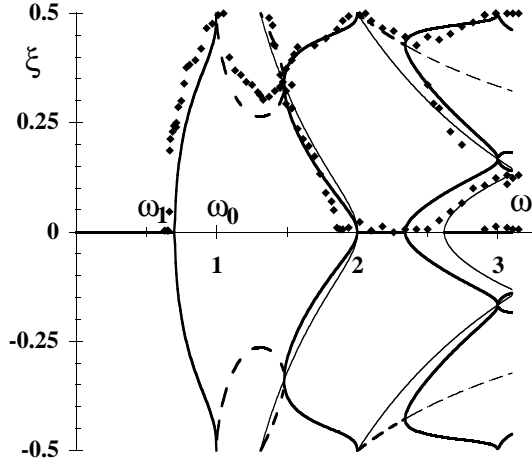


**Fig. 3.** The same diagram as Figure 2 obtained for a light bead ( $m = 0.21$  g and  $\mu = 0.46$ ). The diamonds correspond to the observed equilibrium positions of the bead. The thick continuous lines are the resonance positions (Eq. (12)); the thick dashed lines are the non resonant positions given by equation (14); the thick interrupted lines are the non resonant positions given by equation (15). The three are the predicted stable steady positions. The thin continuous lines correspond to the bead at a vibration node; the thin interrupted lines are given by equation (15). Both represent the unstable steady positions of the bead.

theory, the frequencies are normalized, the fundamental frequency  $\omega_0$  of the string being chosen as unity.

At very low frequency, below any resonance of the system, there is hardly any vibration (amplitude far smaller than 0.5 mm) and the bead has no preferential position. When the frequency approaches a frequency  $\omega_1 = 38$  Hz ( $\omega_1 < \omega_0 = 126$  Hz) the bead is observed to move spontaneously along the wire. This motion has a time scale of 100 s. It is much larger than the vibration time scale which is 0.01 s. Ultimately the bead reaches the middle of the string where it stops sliding. At  $\omega = \omega_1 = 38$  Hz the vibration amplitude has become large (3 mm) and the bead is located at an antinode. Using Helmholtz's results it is possible to compute the frequency of the fundamental mode of the string loaded with the same bead fixed at the center. The resulting value is precisely  $\omega_1$ . This means that the bead has spontaneously moved so as to make the system resonant.

With a fixed bead an increase of the frequency would detune the system. Instead, in the present situation, the bead is observed to leave the center, moving either left or right to a new and well defined position where the vibration amplitude of the whole system remains large. This is a symmetry breaking process: the evolution of  $\xi$  as a function of  $\omega$  in the vicinity of the threshold  $\omega_1$  shows this transition to be a supercritical transition. When  $\omega$  comes close to  $\omega_0 = 126$  Hz, the position of the bead is near one of the extremities of the string. The amplitude of the string vibration is still large (3 mm) but the bead is no longer at an antinode, so that its own motion has a small amplitude (0.5 mm). With a further increase of the frequency, the bead reaches an extremity of the string and

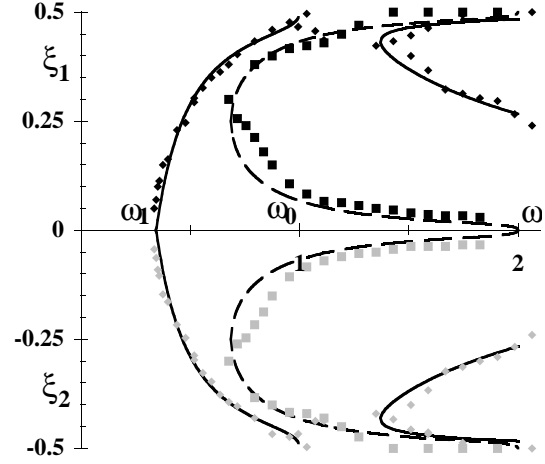


**Fig. 4.** The same diagram as above for the system with two beads. Here the diamonds correspond to the simultaneous positions of the two beads with the homogeneous forcing: one bead (grey symbols) is on the right half of the string, the other (black symbols) is on the left half. The squares were obtained with an antisymmetric excitation of the system. The continuous curves are the predicted resonance equilibrium positions with homogeneous magnetic field given by equation (18). The dashed curves are the predicted resonance equilibrium positions with antisymmetrical magnetic field given by equation (19).

is then at an antinode. The string now vibrates as if there were no bead, with a very large amplitude (5 mm), because this occurs precisely at  $\omega_0 = 126$  Hz, the frequency of the fundamental mode of the string alone. Once again the system has adapted to be resonant.

Above  $\omega_0$ , a second bifurcation occurs. As a result, when  $2\omega_0$  is reached either the bead has returned to the center, or again to one extremity (Fig. 2).

The same experiment done with a bead lighter than the string ( $m = 0.21$  g so that  $\mu = m/\lambda L = 0.46$ , Fig. 3) exhibits mostly the same characteristics. The main difference is that  $\omega_1 = 88$  Hz is larger so that the band of frequencies between  $\omega_1$  and  $\omega_0$  is narrower. The mass is observed to move a larger distance to compensate for a given shift in frequency. Immediately above  $\omega_0 = 126$  Hz, there is a band of frequencies in which, though the bead goes to a well determined position, the system does not appear to be resonant (the vibration amplitudes remain small, of the order of 0.5 mm). For larger frequencies, large amplitudes of vibration are recovered and the equilibrium positions of the bead are similar to the case of the heavier bead.

### 3.2 With two beads

We use the same experimental apparatus but two identical beads are now threaded on the string. The results of such an experiment with each bead having a mass  $m = 0.73$  g ( $\mu = 1.6$ ) are shown in Figure 4. At low frequency, below any resonance, there is hardly any vibration and the beads take no preferential positions. At slightly higher frequencies, the beads move to the middle of the string and stick together. This occurs at the frequency  $\omega_1 = 41$  Hz corresponding to one single bead of mass  $2m$  (and  $2\mu = 3.2$ ).

From there, if the frequency is increased, the beads move in such a way as to stay together and behave as one single bead. However, if the experiment is directly started above the frequency  $\omega_1$ , the following is observed. If the beads are placed on the same half of the string, they move in such a way as to stay together and behave as one single bead. If the beads are placed on different halves of the string, they move to symmetrical positions (Fig. 4). In this case, they will stay symmetrical for any further increase of the frequency.

In the latter case, each bead reaches an extremity of the string when the frequency reaches  $\omega_0 = 126$  Hz. Then they return symmetrically to the center and a supercritical bifurcation occurs: the beads move towards the extremities or the center, remaining in symmetrical positions.

The two beads are not observed to move into the positions expected for the second eigenmode. The reasons, detailed in Section 4.2, lie in the symmetry of the forcing (see Morse [8]). In order to recover the even eigenmodes, we imposed a magnetic field which reverses its sign at the middle of the string. With this antisymmetrical forcing, the beads move to symmetrical positions corresponding to the second eigenmode (Fig. 4), but the odd eigenmodes are no longer excited. In the case of antisymmetrical forcing, the symmetrical positions exist only above a frequency  $\omega_2 = 65$  Hz ( $\omega_2 > \omega_1$ ) where a bifurcation occurs: when the frequency is increased, the beads move either towards the extremities or the center.

## 4 The model and the results

The string equation is the classical wave equation for the transverse displacement  $y$

$$\lambda \partial_{tt} y = T \partial_{xx} y \quad (1)$$

where the  $x$  axis is chosen along the string at rest, the origin is at the center;  $\lambda$  is the string linear density and  $T$  the tension. The  $n$ th eigenmode is defined by its frequency  $\omega_n = n(\pi/L)\sqrt{T/\lambda}$  and its shape  $y = y_0 \sin(n\pi(x/L + 1/2)) \cos(\omega t + \varphi)$ . Here  $L$  is the string length.

### 4.1 With a single bead

If a mass  $m$  is located on the string at  $x = \xi$ , taking into account a forcing  $F \cos(\omega t)$  per unit length, equation (1) becomes

$$(\lambda + m\delta(x - \xi)) \partial_{tt} y = T \partial_{xx} y + F \cos(\omega t). \quad (2)$$

$\delta$  is the Dirac distribution and accounts for the punctual mass. If the bead position changes by  $d\xi$ , the kinetic energy theorem tells us that  $G d\xi = dK$ , where  $G$  is the force acting on the bead, and  $K$  its kinetic energy. The equation of motion reads

$$m \partial_{tt} \xi = \partial_\xi K = \frac{1}{2} m \partial_\xi ((\partial_t \xi)^2 + (\partial_t \eta)^2). \quad (3)$$

Here  $\eta = y(\xi, t)$  is the bead transverse position. Let us note that, of course, a Lagrangian derivation gives the same equations of motion.

We have neglected the gravity  $g$ , as  $mg \sim 0.01$  N is much smaller than the tension  $T = 17$  N. We neglect friction between the bead and the string, it does not change the equilibrium positions. It only contributes to stop the bead at these positions. Moreover, the basic frequency over resonance width ratio is  $\omega_0/\gamma = 25$  so that damping is small. At first, we neglect nonlinearities in string vibration. This assumption will allow us to find the bead positions but not the vibration amplitudes.

We write equations (2, 3) in a non-dimensional form using as units the string length  $L$ , the fundamental frequency  $\omega_0 = (\pi/L)\sqrt{T/\lambda}$  and the time scale  $\tau = \pi/\omega_0$ , therefore

$$(1 + \mu\delta(x - \xi)) \partial_{tt} y = \partial_{xx} y + f \cos(\pi\omega t), \quad (4)$$

$$\partial_{tt} \xi = \frac{1}{2} \partial_\xi ((\partial_t \xi)^2 + (\partial_t \eta)^2). \quad (5)$$

Here  $\mu = m/(\lambda L)$  is the bead/string mass ratio and  $f = FL/T$  the forcing. We have omitted the tildas for the new non-dimensional variables.  $\xi$  varies between  $-1/2$  and  $1/2$ . We look for periodic solutions of the form  $y = Y(x, \xi) \cos(\pi\omega t)$  and  $\eta = \eta_0 \cos(\pi\omega t)$  (we drop the phase since there is no damping) so

$$-\pi^2 \omega^2 (1 + \mu\delta(x - \xi)) Y = \partial_{xx} Y + f. \quad (6)$$

When  $f = 0$ , equation (6) is a Schrödinger equation for a particle in a box with a short range potential, the so-called quantum billiard with a point-like scatterer [3]. Since  $\xi$  is only a function of time,  $\partial_\xi (\partial_t \xi)^2 = 0$ . Therefore, equation (5) averaged in time gives the slow dynamics of the bead steady position  $\xi$ :

$$\partial_{tt} \xi = \frac{\pi^2}{4} \omega^2 \partial_\xi \eta_0^2. \quad (7)$$

Thus, the dynamics is that of a bead moving in a potential  $-\pi^2 \omega^2 \eta_0^2(\xi)/4$ , and the behaviour of  $(\eta_0(x))^2$  gives the equilibrium positions and their stability. We look for solutions of (6) of the form

$$Y(x, \xi) = \frac{f}{\pi^2 \omega^2} (\cos \pi\omega(x + 1/2) - 1 + A \sin \pi\omega(x + 1/2)) \quad \text{if } x < \xi,$$

$$Y(x, \xi) = \frac{f}{\pi^2 \omega^2} (\cos \pi\omega(x - 1/2) - 1 + B \sin \pi\omega(x - 1/2)) \quad \text{if } x > \xi, \quad (8)$$

fulfilling the boundary conditions  $Y(-1/2) = Y(1/2) = 0$ .  $A$  and  $B$  are determined by the conditions

$$Y(\xi^+, \xi) = Y(\xi^-, \xi), \quad (9)$$

$$-\pi^2 \omega^2 \mu Y(\xi, \xi) = \partial_x Y(\xi^+, \xi) - \partial_x Y(\xi^-, \xi), \quad (10)$$

the first condition imposes continuity at  $x = \xi$ , the second comes from integration of (6) between  $\xi - \varepsilon$  and  $\xi + \varepsilon$  in the limit  $\varepsilon \rightarrow 0$ . The discontinuity in the string slope (see Fig. 5) is due to the bead infinite inertia per unit length.

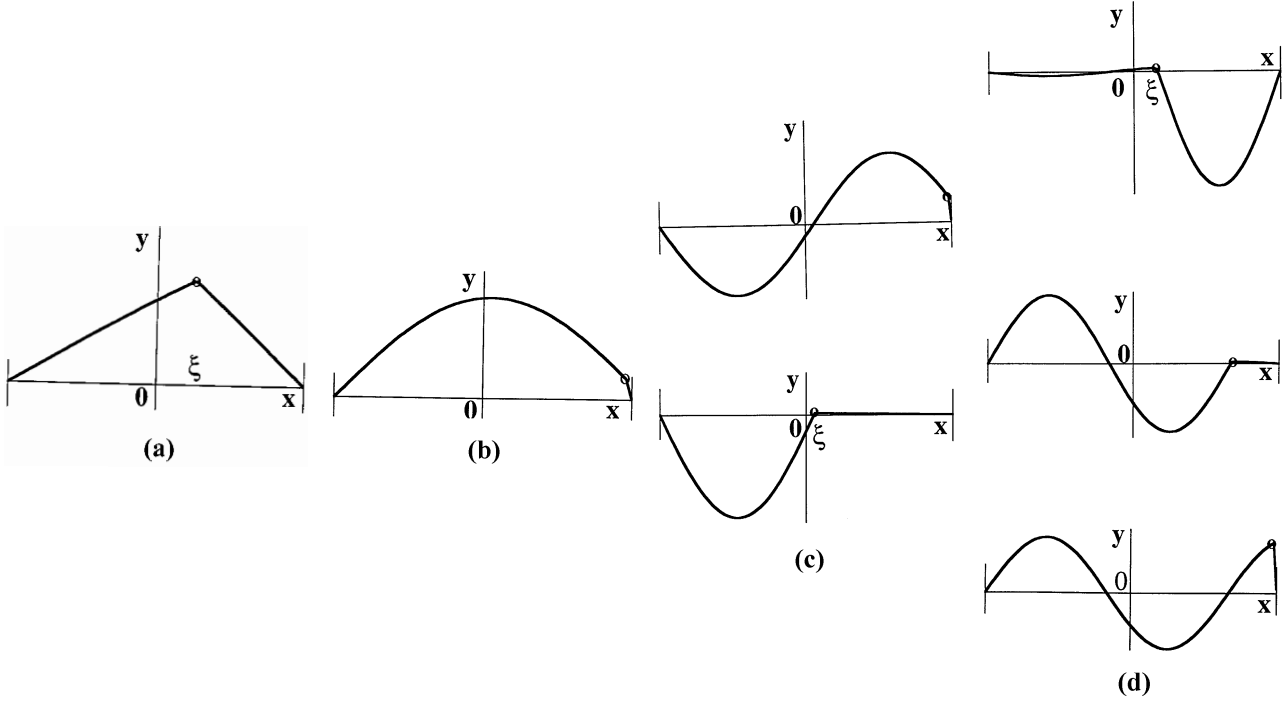


**Fig. 5.** The string shapes obtained theoretically for  $\mu = 4.0$  at different values of the nondimensional frequencies  $\omega$ . Note that the beads generate a slope discontinuity. The amplitude units are arbitrary and are magnified to show clearly the strings shapes. The experimental amplitudes are of the order of 5 mm, the string length being 30 cm. (a) At  $\omega = 0.31$ , the system is just above the first bifurcation and the bead is at the antinode. (b) At  $\omega = 0.95$ , there is one equilibrium position near a node. (c) The two possible solutions for  $\omega = 1.9$ . In both, the bead is near a node. (d) The three possible solutions at  $\omega = 2.4$ .

We compute  $A$  and  $B$  in equation (8) using the conditions (9, 10) to find the amplitude of vibration of the bead at  $\xi$ :

$$\begin{aligned} \eta_0(\xi) &= Y(\xi, \xi) \\ &= \frac{f}{\pi^2 \omega^2} \left( \frac{2 \sin(\pi\omega/2) \cos(\pi\omega\xi)}{\sin(\pi\omega) + \pi\omega\mu \cos^2(\pi\omega/2) - \pi\omega\mu \cos^2(\pi\omega\xi)} - 1 \right). \end{aligned} \quad (11)$$

One can easily determine the bead equilibrium positions and their stability. First, the positions where  $\eta_0(\xi) = \pm\infty$  are given by

$$\sin(\pi\omega) + \pi\omega\mu \cos^2(\pi\omega/2) - \pi\omega\mu \cos^2(\pi\omega\xi) = 0. \quad (12)$$

These curves are plotted in Figures 2 and 3 for two different values of  $\mu$  ( $\mu = 4.0$  and  $\mu = 0.46$ ).

We can now revisit the system with the bead fixed at a position  $\xi_f$ . For each position  $\xi_f$ , Helmholtz's calculations [2] give, with our notations, the eigenfrequencies  $\omega_f$ , *i.e.* the frequencies at which the amplitudes deduced from the linear string equation (2) are infinite:

$$\sin(\pi\omega_f) = \pi\omega\mu \sin(\pi\omega_f(\xi_f + 1/2)) \sin(\pi\omega_f(\xi_f - 1/2)). \quad (13)$$

The resulting curves  $\omega_f(\xi_f)$  are identical to the curves  $\omega(\xi)$  given by equation (12). Thus, the slow dynamics of our system leads it to self-tuning at a resonance. This is observed experimentally: when the bead has reached its

steady position, the system as a whole has a maximum amplitude of vibration (limited in practice to about 3 mm because of the non-linearities). When the bead reduced mass is large ( $\mu = 4$  in Fig. 2) the system is resonant at almost any imposed frequency. With a light bead ( $\mu = 0.46$  in Fig. 3) the resonance spectrum shows bands separated by gaps with no possible resonance. When  $\mu \rightarrow 0$ , we recover the simple string with resonances only at  $\omega = 1, 2, 3 \dots$

Equation (8) gives the shape of the string once  $A$  and  $B$  computed. For each frequency (in order of increasing values) we look for the possible positions of the bead for which the system is at resonance. The lowest possible frequency of the system ( $\omega_1 = 0.3$  for  $\mu = 4$ ) is found when the bead is at the center of the string, at the antinode of the fundamental mode. Between  $\omega_1$  and the basic frequency  $\omega_0$  of the unloaded string only one position  $\xi$  of the bead (and its symmetric  $-\xi$ ) can provide a resonance. Close to  $\omega_1$ , just above the first bifurcation, the resonant positions correspond to the bead slightly off-centered and still at a vibration antinode as shown in Figure 5a ( $\omega = 0.31$ ). Closer to  $\omega_0$  ( $\omega = 0.95$  in Fig. 5b) the bead is close to an extremity of the string and no longer at an antinode. At  $\omega_0$  the bead reaches the node located at the string end. Between  $\omega_0$  and  $2\omega_0$ , two distinct values of  $\xi$  (and their symmetric) can give resonances. This corresponds to the second bifurcation of the system. The shapes of the string are shown for  $\omega = 1.9$  in Figure 5c. For

frequencies between  $2\omega_0$  and  $3\omega_0$ , there are three distinct solutions with shapes shown in Figure 5d for  $\omega = 2.4$ .

There is usually a discontinuity of the string slope at the bead, the only exception being the bead located exactly at a node. The bead is at an antinode, or close to it, in the lower frequency range. In all other cases it remains close to a node. All these predicted shapes of vibrations correspond exactly to those observed experimentally. As noted above, with a homogeneous forcing, the mode two of a vibrating string should not be excited. Here, because the introduction of a single bead has broken the symmetry, it becomes possible.

When the bead is light (Fig. 3) there are frequencies for which no position of the bead can give a resonance. These frequencies form gaps of values separating the bands where there is resonance. Experimentally however, when the system is excited at such a frequency, the bead is still observed to choose a well defined position and to stay there.

This behaviour can be understood by noting that setting  $\partial_{\xi}\eta_0 = 0$  in equation (11) gives additional equilibrium positions of the bead. These are absent in Helmholtz theory since they do not correspond to resonances. These positions are those that are observed here in the gaps. They are determined by two equations:

$$\sin(\pi\omega) + \pi\omega\mu \cos^2(\pi\omega/2) + \pi\omega\mu \cos^2(\pi\omega\xi) = 0, \quad (14)$$

$$\sin(\pi\omega\xi) = 0. \quad (15)$$

All the different types of solutions are shown in Figure 4. At the intersections of the curves resulting from equations (12, 14, 15), there are bifurcations with exchange of stability (Fig. 4). The solutions of (14, 15) (Fig. 2) are stable only in the gaps. The observed bead positions (Fig. 4) agree with predictions. The slight discrepancies can be attributed to the weak inhomogeneity of the magnetic field  $B$  along the string. When this inhomogeneity is made voluntarily larger, these discrepancies are increased.

#### 4.2 With two beads

The observations done in continuous systems (soap films or smectic films) show a trend for the system to adapt by concentrating mass at the antinodes. This is observed in the one-bead system only at the lower frequencies. It appears that one single bead can be close to an antinode when there is only one antinode. For the higher modes, if the bead were to be at one of the antinodes, it would cause this antinode to completely differ from the others, and thus destroy the possibility of a resonance. If  $n$  beads were placed at the  $n$  antinodes of the  $n$ th eigenmode, the system would be tunable by a bifurcation similar to the bifurcation observed with one antinode in the one-bead system. The analogy with continuous systems was the motivation for the investigation of the string loaded with two beads.

But with two beads, the system acquires two extra degrees of freedom. For this reason, one expects the resonance condition to be some function  $g_{\omega}(\xi_1, \xi_2) = 0$  of the beads horizontal positions; so the set of equilibrium positions should be infinite. However, the experiment shows

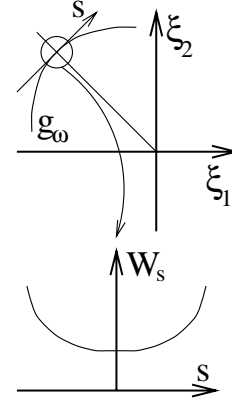


**Fig. 6.** Schematic plot of the resonance function  $g_{\omega}(\xi_1, \xi_2) = 0$  near a symmetric resonant position  $(-\xi, \xi)$ . This graph is symmetric with respect to the line of equation  $\xi_1 = \xi_2$ . A sketch of the stretching energy  $W_s$  along the tangent is shown.

that there is only a finite number of steady positions for each frequency. Therefore there must be a selection process.

The selection process seems to be linked to the limitations in the amplitudes of oscillations. In fact, the amplitude of vibration is determined by nonlinearities and not by damping. The observed amplitudes of the string motion at the antinodes in our experiment is  $A \leq 5$  mm. If it were due to damping, we would have  $A/L \approx FL\omega_0/(T\gamma)$  with  $F = IB$  the magnetic force,  $L$  the string length,  $\omega_0$  the fundamental frequency,  $T$  the string tension and  $\gamma$  the resonance width. So the amplitude would be  $A \sim 6$  cm, which is much greater than the experimental amplitude. Hence, we have to take into account string stretching, elastic bending and geometrical nonlinearities hidden by equation (1). A rough estimate shows that stretching is dominant and from Morse [9], equation (1) becomes

$$\lambda\partial_{tt}y = T\partial_{xx}y + \frac{1}{2}Es\partial_x((\partial_x y)^3) + F\cos(\omega t) \quad (16)$$

where  $E \sim 2 \times 10^{11}$  N.m<sup>-2</sup> is the steel Young modulus and  $s$  the string cross section. The cubic term stands for the elastic restoring force due to the string extension while vibrating. From equation (16), we estimate  $F \approx Es/L(A/L)^3$  so that  $A \sim 5$  mm, which is consistent with the experiment. So, the new ingredient is the stretching energy  $W_s$ . In terms of the dimensionless variables, it reads

$$W_s(\xi_1, \xi_2) \approx \frac{1}{8}EsL \int_{-1/2}^{1/2} (\partial_x Y)^4 dx. \quad (17)$$

In fact we will not use this expression but we will only use its symmetries in the beads positions. Figure 6 shows the plane  $(\xi_1, \xi_2)$  where the symmetries are explicitied. Note that the system is invariant by the permutation  $(\xi_1, \xi_2) \rightarrow (\xi_2, \xi_1)$ , the symmetry with respect to the string middle  $(\xi_1, \xi_2) \rightarrow (-\xi_1, -\xi_2)$  and so is  $W_s$  and the function  $g_{\omega}(\xi_1, \xi_2)$ . We hereafter consider the vicinity of a resonant position  $(-\xi, \xi)$ . The invariance by the transformation

$\Psi: (\xi_1, \xi_2) \rightarrow (-\xi_2, -\xi_1)$  shows that, at  $(-\xi, \xi)$ , the curve  $g_\omega(\xi_1, \xi_2) = 0$  has a tangent parallel to the line of equation  $\xi_1 = \xi_2$  and a parameterization  $\xi_1 = -\xi + s$ ,  $\xi_2 = \xi + s$  (Fig. 6). The invariance by  $\Psi$  shows that  $W_s$  is even with respect to  $s$ :  $W_s(-\xi + s, \xi + s) = W_s(-\xi - s, \xi - s)$ . Thus, along the tangent,  $W_s(-\xi + s, \xi + s)$  has a maximum or a minimum for  $s = 0$ . The experiment shows that it is actually a minimum, *i.e.* the stretching energy is minimum for the resonant position  $(-\xi, \xi)$ . Of course, one could make the cumbersome calculations with the stretching energy expression to find that the symmetric positions are selected. Our intention was only to show how to guess the solutions by only considering the symmetries in the beads' positions.

The symmetry with respect to the string middle suggests looking for the beads positions with  $\xi_1 = -\xi_2$  among the resonant positions defined by  $g_\omega(\xi_1, \xi_2)$ . Now we have a single variable ( $\xi_1 = -\xi_2$ ). The calculations are very similar to those in Section 4.1.

For the odd eigenmodes, the string shape is symmetrical and the beads' equilibrium positions are  $(-\xi, \xi)$ ,  $\xi > 0$ , where

$$\pi\omega\mu \sin \pi\omega(2\xi - 1/2) = \pi\omega\mu \sin(\pi\omega/2) - 2 \cos(\pi\omega/2). \quad (18)$$

This curve is plotted in Figure 4. The experimental positions agree with the theoretical ones. The beads' positions are symmetric and correspond to resonance.

For the even eigenmodes, the string shape is antisymmetrical and the beads' positions are defined by

$$\pi\omega\mu \cos \pi\omega(2\xi - 1/2) = \pi\omega\mu \cos(\pi\omega/2) + 2 \sin(\pi\omega/2). \quad (19)$$

These positions are plotted in Figure 4 and agree with the experimental positions obtained with the antisymmetrical configuration of the magnetic field. Again, the two beads are in symmetric positions.

These positions are not observed with a homogeneous forcing, because it is symmetric with respect to the string middle. Morse [8] shows that the string eigenmodes of antisymmetrical shape are not excited when the forcing is homogeneous. We believe the argument of symmetry given above offers an interpretation of a result that surprised Morse.

## 5 Conclusion

In summary, we have shown that a string with one or two sliding beads adapts itself to become resonant at the forcing frequency through a slow dynamics process. There is a dramatic change in the nature of the system with additional degrees of freedom. While the single string has a discrete resonance spectrum, the string with a sliding bead acquires a continuous one. As a consequence, the beaded string responds to the forcing with a large amplitude within a whole range of frequencies.

In a forthcoming article [10], we will focus on the evolution of mass distribution as the key to the self-adaptative

behaviour of thick vibrating soap films. The large thickness at an antinode corresponds to a concentration of mass; so that it could be modelled by a bead at antinode. Therefore, an equivalent for the soap film with  $n$  antinodes, would be a string loaded with  $n$  beads and excited in the  $n$ th eigenmode. The soap film would be tunable through bifurcations similar to the first bifurcation observed with the string loaded with two beads in the case where the beads separate from each other.

For solid membranes, the vibration modes are often visualised by spreading sand on their surface (Chladni figures [11]). Self-adaptation would presumably be observed if the sand mass was comparable to the membrane mass. Similarly, as there are many systems which obey the string equation, self-tuning could be obtained in systems such as acoustical, microwave or optical cavities having more practical interest. In the last two cases the radiation pressure acting on a dielectric could generate the slow dynamics.

The authors thank M. Brazovskaia and P. Pieranski for fruitful discussions and for sending them their preprint prior to publication, and E. Corvera Poiré for a critical reading of the manuscript and useful comments.

## References

1. J.-L. Lagrange, *Œuvres* (Gauthier-Villars, Paris, 1867), Vol. I, p. 59.
2. H.V. Helmholtz, *Vorlesungen über Theoretische Physik* (Ambrosius Barth, Leipzig, 1908), Vol. III, p. 139. A more accessible reference is J.W. Rayleigh, *The Theory of Sound* (Dover publications, New York, 1945), p. 204.
3. M. Brazovskaia, P. Pieranski, *Phys. Rev. Lett.* **80**, 5595 (1998).
4. M. Airiau, *Étude des vibrations des membranes de savon*, DEA Report, ENS, Paris, 1986.
5. M. Brazovskaia, H. Dumoulin, P. Pieranski, *Phys. Rev. Lett.* **76**, 1655 (1996).
6. P. Pieranski, L. Belliard, J.-Ph. Tournellec, X. Leoncini, C. Furtlehner, H. Dumoulin, E. Riou, B. Jouvin, J.-P. Fénerol, Ph. Palaric, J. Heuvig, B. Cartier, I. Kraus, *Physica A* **194**, 364 (1993).
7. Preliminary experiments were performed using a thick cylindrical rubber string. The bead was a Teflon cylinder. The hole in the center was just a little larger than the string diameter and the intermediate space was filled with oil so that the friction between the two was of a viscous type. The same behaviour of self-adaptation was observed. This setup was abandoned as the control of the mechanical forcing was less precise, and because some additional difficulties arose from the slow time evolution of the rubber's elastic properties.
8. P.M. Morse, *Vibration and Sound* (McGraw Hill, New York, 1936), p. 94.
9. P.M. Morse, K.V. Ingard, *Theoretical Acoustics* (McGraw Hill, New York, 1968), p. 856.
10. A. Boudaoud, Y. Couder, M. Ben Amar, *Self-adaptation in vibrating soap films*, *Phys. Rev. Lett.* (submitted).
11. M. Faraday, *Philos. Trans. Roy. Soc. London* **52**, 299 (1831).